



## Diurnal to interannual variability in the Northeast Atlantic from hydrographic transects and fixed time-series across the Rockall Trough

Eoghan Daly<sup>a,\*</sup>, Glenn Nolan<sup>a</sup>, Alan Berry<sup>a</sup>, Janina V. Büscher<sup>b</sup>, Rachel R. Cave<sup>b</sup>, Levke Caesar<sup>c</sup>, Margot Cronin<sup>a</sup>, Sheena Fennell<sup>b</sup>, Kieran Lyons<sup>a</sup>, Aedín McAleer<sup>b</sup>, Gerard D. McCarthy<sup>c</sup>, Evin McGovern<sup>a</sup>, Joseph V. McGovern<sup>a</sup>, Triona McGrath<sup>d</sup>, Garvan O'Donnell<sup>a</sup>, Diego Pereiro<sup>a</sup>, Rob Thomas<sup>a</sup>, Louise Vaughan<sup>a,e</sup>, Martin White<sup>b</sup>, Caroline Cusack<sup>a</sup>

<sup>a</sup> Marine Institute, Rinville, Oranmore, Co, Galway, Ireland

<sup>b</sup> University of Galway, University Road, Galway, Ireland

<sup>c</sup> National University of Ireland, Maynooth, Co, Kildare, Ireland

<sup>d</sup> An Fóram Uisce, Limerick Road, Nenagh, Co, Tipperary, Ireland

<sup>e</sup> Atlantic Technological University, Dublin Road, Galway, Ireland

### ARTICLE INFO

#### Keywords:

Rockall Trough  
Northeast Atlantic  
Water column variability  
Hydrographic time-series  
Water mass modification  
Boundary currents

### ABSTRACT

The southern entrance to the Rockall Trough is subject to a complex set of dynamic processes, influenced by Atlantic gyre interactions, the North Atlantic Current, slope boundary currents, variable wind stress forcing, mesoscale activity, and a changing supply of modified water masses formed elsewhere in the Atlantic. These processes drive large temporal and spatial variations, and mixing of surface and intermediate water mass properties that advect through the Trough and drive variations in the deeper waters circulating around it. Here, we investigate variability across the southern and central Rockall Trough from standard hydrographic sections (2006–2022) and deepwater moored subsurface measurements, to better understand changes in water column characteristics and water mass modification during advection through the Rockall Trough and track the aftermath of recent freshening events. Rapid and longer-term physical changes are assessed along with spatial variability and watermass interaction. Interannual variability is large across intermediate depths, deeper circulations are regenerated and a salinity core associated with the eastern boundary current is detailed. Establishing, maintaining, monitoring and analysis of observational ocean time-series datasets are a fundamental requirement for managing and conserving crucial biological resources and are key to understanding oceanic and earth system change.

### 1. Introduction

The Rockall Trough (hereafter: RT), located in the northeast North Atlantic, is an elongated deepwater channel shallowing from the southwest to northeast (Fig. 1). Opening at > 3500 m, through-flow is capped at ~600 m across the Wyville-Thomson Ridge to the northeast and at ~1200 m to the north, between the banks of George Bligh and Lousy, restricting most deeper waters to recirculate around the trough (Holliday et al., 2000). The channel is bounded to the east by the Porcupine Bank and the Irish and Hebridean shelves along the European continental margin and flanked to the west by features of the Rockall Plateau, such as the Rockall Bank and the Feni Ridge. The RT provides an important transport pathway for heat and salt from

upper/intermediate water masses advecting from the wider North Atlantic into the Nordic Seas (Ellett et al., 1986; Pingree, 1993; New et al., 2001). While the hydrography of the region is very well described (e.g. Ellett and Martin, 1973; New and Smythe-Wright, 2001; Holliday and Cunningham, 2013), finer details of the processes involved, including long-term trends and natural oscillations, are still topics of debate.

The South Rockall Trough (hereafter: SRT), at the opening of the channel, through which the main transect of this study spans, is a very dynamic area in terms of its oceanography. It experiences hydrographic variability across a range of scales, dictated by a complexity of oceanographic processes, and notable for its varied collection of water masses (Fig. 1A). Most water masses throughout the water column in the RT are

\* Corresponding author. Rinville, Oranmore, Co, Galway, H91 R673, Ireland.  
E-mail address: [eoghan.daly@marine.ie](mailto:eoghan.daly@marine.ie) (E. Daly).

<https://doi.org/10.1016/j.dsr.2024.104233>

Received 12 June 2023; Received in revised form 15 December 2023; Accepted 4 January 2024

Available online 14 January 2024

0967-0637/© 2024 The Authors. Published by Elsevier Ltd. This is an open access article under the CC BY license (<http://creativecommons.org/licenses/by/4.0/>).

sourced remotely and arrive modified through a number of transport processes and pathways. Below the surface mixed layer, the prevailing upper-intermediate water mass is Eastern North Atlantic Water (ENAW; Harvey, 1982; also known as Eastern North Atlantic Central Water or ENACW; Mauritzen et al., 2001). The warm and saline ENAW is described as occupying salinities of  $\pm 0.05$  from a mixing line between 12 and 4 °C and 35.66–34.96 in potential temperature–salinity ( $\theta$ - $S$ ) space, with a slight fresh inflexion at  $\sim 9.4$  °C (Harvey, 1982). ENAW is formed in the Bay of Biscay as a mode water (Pollard et al., 1996), yet influenced at source by underlying Mediterranean water, which will cool and freshen to a modified state, as it advects north and into the RT. ENAW advection continues over the Rockall Plateau and Trough, to at least 57–59°N, staying mostly east of 20°W at upper/intermediate depths >300 m, at the opening of the RT (52.5°N, 20°W) (Ellett and Martin, 1973; Wade et al., 1997).

Along the eastern extent of the Sub-Polar Front (SPF), Subarctic Intermediate Water (SAIW) enters the SRT region as a relatively cold, fresh and very stratified intermediate water mass. Having been formed within the Sub-Polar Gyre (SPG) from the fresh surface waters of the Labrador Sea (i.e. not considered a mode water), SAIW proceeds to subduct beneath the SPF travelling east along the northern flank of the North Atlantic Current (NAC) (Arhan, 1990; Wade et al., 1997). SAIW is characterised by temperatures of 8–9 °C and salinities of 35.1–35.2 at depths between 600 and 1000 m in the RT (Ullgren and White, 2010), with a salinity minimum at potential density anomaly ( $\sigma_\theta$ ) of 27.3 kg m<sup>-3</sup> (Harvey and Arhan, 1988). Although not always as evident in the RT, McGrath et al. (2012) identified SAIW as a water mass with relatively high nutrients and oxygen, with a relatively low Apparent Oxygen Utilisation (AOU) along the western side of SRT (>18°W) in 2008 and 2009, and a stronger more central signature in 2010.

Mediterranean Overflow Water (MOW) having rapidly mixed with local North Atlantic water outside the Strait of Gibraltar off southern Spain, spreads westward (Needler and Heath, 1975) and northwards, as a very saline and warm water mass (>11.4 °C; >36, at source) (Perez

et al., 1993; Arhan et al., 1994; Arhan and King, 1995 and references within). MOW reaches the SRT as a relatively warm and very saline tongue ( $\sigma_\theta \sim 27.6$  kg m<sup>-3</sup>, Ullgren and White, 2010; depth 700–1000 m, temperature  $\geq 9.12$  °C, salinity  $\geq 35.32$ ; McGrath et al., 2012), at least as far as 53°N (McCartney and Mauritzen, 2001). The most direct pathway described for MOW into the RT is along the Eastern Boundary Current (EBC) system (e.g. Reid, 1979; Smilenova et al., 2020), and more indirectly through northward advection, interacting with the SPF and mixing with the central waters of the Sub-Tropical Gyre (STG; e.g. Iorga and Lozier, 1999; Mauritzen et al., 2001; Bower et al., 2002). MOW may become blocked from entering the RT during times of an expanded SPG, which will deliver the more stratified SAIW across the trough as far as the eastern slope (Lozier and Stewart, 2008).

Underlying the assortment of intermediate water masses vying for dominance at the entrance to the Rockall Channel is the cool and very fresh Labrador Sea Water (LSW). Having formed through deep water convection along the southwest bounds of the Labrador Sea, LSW transits eastward (among other pathways), as a deep component of the SPG (Talley and McCartney, 1982; Yashayaev et al., 2007, 2008). LSW can be seen as either of two modes, upper or deep (Yashayaev et al., 2007; Kieke et al., 2009), depending on how extreme the winter convection conditions were, at formation. New pulses of LSW periodically or occasionally enter the RT to regenerate the background recirculation of LSW within (Holliday et al., 2000). Beneath LSW lies Northeast Atlantic Deep Water (NEADW), which overlies Lower Deep Water (LDW) and/or Antarctic Bottom Water (AABW) (McCartney, 1992; van Aken, 2000, and references within), each of which are very limited by topography to the southern extents of the trough. Other water masses will enter the RT and influence, to a lesser degree, the water mass balance present at SRT, such as Western North Atlantic Water (WNAW) occasionally replacing ENAW from the west (Pollard et al., 1996). The very cold ( $\sim 0$  °C) Nordic Sea outflow of Wyville-Thompson Overflow Water (WTOW) warms along its limited journey south in the western RT, along the Feni Ridge, at least as far as 55°N (Sherwin et al., 2008; Johnson et al., 2010).

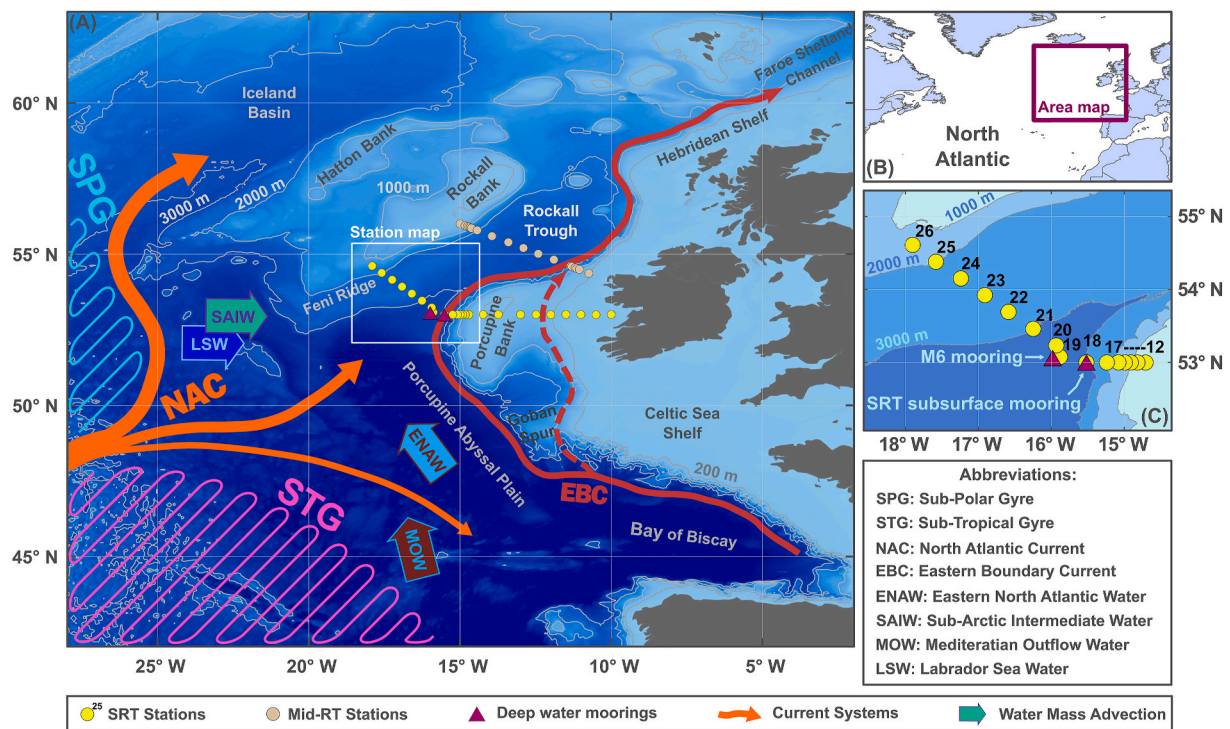


Fig. 1. Area map (A), displaying the South Rockall Trough (SRT) transect (yellow circles per station), Mid Rockall Trough (grey circles) and fixed moorings (purple triangles). The Sub-Polar and Sub-Tropical Gyres are indicated with light blue and pink hatching respectively. Please note, current and water mass pathways (see key and abbreviations) are indicative only. They do not convey actual positions, nor reflect spatial variation or changes in direction over time. The overview map (B) regionally displays the area map (purple polygon) within the northern North Atlantic. Station map (C) shows station numbers and locations of the SRT transect.

WTOW was confirmed through relatively high oxygen content, to be limited to the western flank, between 800 and 1100 m at  $\sim 56^\circ\text{N}$ , in 2009 and 2010 (McGrath et al., 2012).

SPF position and flow characteristics of the NAC, resulting from gyre expansion and contraction, will have direct downstream influences on the properties and proportions of water masses passing through the RT at all but the deepest depths. The interplay between the two North Atlantic gyre systems (Schmitz and McCartney, 1993; Arhan et al., 1994; Johnson et al., 2013; Hátún et al., 2016; Nowitzki et al., 2021), directing the branched flow paths of the NAC east of the Mid Atlantic Ridge (e.g. Belkin and Levitus, 1996; Hátún et al., 2005; Stendardo et al., 2020) are predominantly dictated by atmospheric oscillations (Hurrell, 1995; Dickson et al., 1996; Pingree, 2002) and wind stress fields (Marshall et al., 2001; Holliday et al., 2020). These oscillations, along with long-term trends, are imbedded in the large interannual to decadal variability in the RT (Holliday et al., 2000; Holliday, 2003), the eastern North Atlantic (Holliday et al., 2015) and in the globally connected Meridional Overturning Circulation (MOC) (Häkkinen et al., 2011; McCarthy et al., 2018; Caesar et al., 2021; Jones et al., 2023).

In addition to the larger scale transporters of water to the RT, the Eastern Boundary Current system (also known as the European slope current or the shelf edge current, among other names) delivers warm and saline water along the European continental margin and on into Nordic Seas. The current is seasonal, being strongest in autumn (September, October (SO); Pingree et al., 1999) or winter (Souza et al., 2001), with a weakening and/or flow reversals in early spring (March, April (MA); Pingree et al., 1999). Proposed drivers for the current system include meridional pressure gradient differences between the shelf and ocean (JEBAR; Huthnance, 1984), density gradient forcing (Booth and Ellett, 1983; Pingree and Le Cann, 1989) and wind stress curl (Orvik and Skagseth, 2003). Transports and current speeds vary greatly (Holliday et al., 2000; Xu et al., 2015) and the flow along the SRT may not manifest as a single jet like stream, rather through a series of shelf and deep currents, with potential under currents or counter currents (Moritz et al., 2021; Fraser et al., 2022).

Mesoscale activity in the wider region and within the RT, will blur any water mass signals in the data. Cold-core eddies can spin off the SPF and enter the trough as the NAC turns north (Wade et al., 1997), while semi-permanent rotations are also found in long-term datasets (e.g. Xu et al., 2015; Moritz et al., 2021). Smilenova et al. (2020) describe a permanent anticyclonic eddy located in the mid-RT, maintained by MOW rich sub-vortices spinning off the boundary current, while Xu et al. (2015) note a seasonal reversal (cyclonic in winter and strongly so in autumn) in velocity anomalies around the same feature, along with seasonality in flow along the margin. Eddies both enter and are formed at the Goban Spur region, from branches of the NAC and from boundary currents respectively (Moritz et al., 2021). These add to the complexity of water mass variation and ultimately smudge any distinct advection signals moving into the RT.

In this paper we will present time-series data and their methods of acquisition across this most dynamic region at the opening of the RT, over the last decade and a half. Observations are then discussed in the context of the above described processes, interactions and variability of water masses on their journey circulating throughout the region.

## 2. Methods and data

To gauge RT variability, two data sources are used: hydrographic transects and fixed mooring time-series; for measuring, monitoring and ultimately understanding the changes seen in this region of the eastern North Atlantic. The primary dataset presented here was obtained from repeat hydrographic transects (Fig. 1A–C), carried out by the Marine Institute of Ireland, on-board the R.V. Celtic Explorer. These ‘Ocean Climate’ cruises began in 2006 and have been ongoing for most years in winter, with occasional years and stations missing due to adverse weather conditions (Fig. 2 shows a table of stations and years occupied)

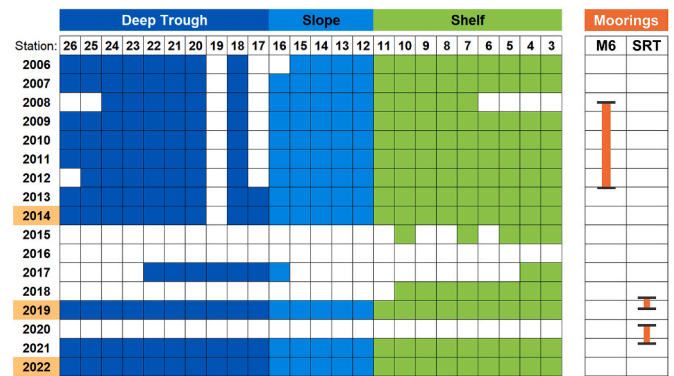


Fig. 2. Station occupation table displaying which SRT stations received CTD casts and in which years, with orange background years denoting surveys that took place in spring (A,M,J), where all other years took place in winter (J,F,M). Mooring deployments are delineated using orange bars, with M6 being the met buoy located adjacent to station 19 and SRT being the South Rockall Trough subsurface mooring located approximately at station 18.

and are presented here in full for the first time. Deepwater moored instruments provide Eulerian or fixed measurement CTD data from deployments of two deep water (>3000 m) moorings (Fig. 1C; purple triangles) on the continental margin at  $53^\circ\text{N}$ .

### 2.1. Data acquisition

The SRT CTD transect of standard stations lies in a northwest-southeast direction across the deep trough and extends eastward, in shallow waters <200 m, across the European continental shelf at  $53^\circ\text{N}$  (Fig. 1A–C; yellow dots are standard CTD stations). Essential Ocean Variables (EOVs) collected at occupied SRT CTD stations include temperature, salinity, dissolved oxygen (since 2010; McGrath et al., 2012) and a comprehensive suite of biogeochemical variables (e.g. nutrients, since 2013). Further north, a CTD transect across the mid-RT was discontinued after 2013 (Fig. 1A, grey dots). All scientific cruises employed a Seabird SBE911plus CTD system and rosette of Niskin bottles, with salinity calibrated from bench water samples analysed on a Guildline Portasal salinometer for some years. Dissolved oxygen was measured using a factory calibrated Seabird SBE43 sensor.

As part of the Irish Marine Data Buoy Observation Network, the deepwater meteorological buoy (the M6 buoy: currently at  $53^\circ\text{N}$ ,  $15.9^\circ\text{W}$ ; Fig. 1C, purple triangle) became operational in 2006. During a period between late 2008 and early 2013, there were subsurface CTD sensors (SeaBird SBE37 MicroCATs, sampling hourly) deployed on the M6 mooring string at depths of 250, 500, 750 and 1000 m, with only short gaps in the data over that period for swap-outs or instrument failure. Since 2018, an additional subsurface only mooring has been deployed close by the M6 buoy ( $\sim 28$  km to the east at  $53^\circ\text{N}$ ,  $15.5^\circ\text{W}$ ; Fig. 1C, purple triangle). This SRT subsurface mooring comprises a number of SBE37s (between 7 and 10 depending on which deployment, all sampling half-hourly) from 1000 m down to the bottom at  $\sim 3200$  m. The SRT subsurface mooring also includes an upward looking ADCP (presently at 1000 m) swapping between an RDI Longranger, 75 kHz and a Nortek Signature 55 kHz, per deployment. In 2022, following many issues, such as the mooring being dragged and snapped below the ADCP, the subsurface mooring was declared operational, with future plans to sustain this observatory as an EMSO Regional Facility site.

### 2.2. Processing, quality control and analysis

All shipboard and fixed CTD data have been processed and quality controlled using a Python architecture on a Jupyter Notebook platform. In the case of shipboard CTD data, a newly developed Notebook utilises Seabird Data Processing software for the main processing steps, while

adding customisable oxygen alignment and heave compensation values on its front-end. Additional Notebooks include calibration from bench values of salinity and oxygen, parameter despiking, range checks and a visual quality control utility, before archiving to a structured database. The fixed CTD Notebooks include a suite of processing/quality control steps similar to above. Transect datasets are freely available through the Marine Institute's ERDDAP page: <https://erddap.marine.ie/erddap/index.html>.

The ship-based hydrographic transect has only just become mature enough to be considered a time-series; defined as over 10 years by the ICES Report on Ocean Climate (Gonzalez-Pola et al., 2022). For the purposes of this paper, a winter climatology is built from all years available. The climatology consists of vertically averaged 5 m bins throughout the water column at each station across all 10 winter (Jan–Mar) transects occupied between 2006 and 2022 (Fig. 2). Anomalies are simply the difference between the depth averaged *in-situ* values collected each year and the long term average value, or climatology. January to March was considered as winter since they were the coolest months at all upper/intermediate depths gleaned from a curve of averaged (depth and station) monthly temperature values extracted from the CMEMS 'Iberia Biscay Irish (IBI)' ocean model at the SRT station locations (and following e.g. Wade et al., 1997; Holliday, 2003; Sherwin et al., 2012). An attempt was made to include spring cruises (2014, 2019, 2022) in the analysis using a model to adjust for the seasonal bias, but these years ultimately had to be excluded from the winter climatology. This is because analyses using the IBI reanalysis product (Aznar et al., 2016; <https://doi.org/10.48670/moi-00029>), showed that modelled data, although representative, lacked accuracy in water column structure to robustly deseasonalise the data.

Fixed mooring data were extrapolated through linear interpolation to 20 m bins from hourly sampled instrument data at nominal depths of 250, 500, 750 and 1000 m. Interpolation took place over a rolling two-day period to take advantage of the instruments' continuously varying *in-situ* depths due to ocean currents or 'knockdown' and to remove any tidal aliasing.

### 3. Results

#### 3.1. CTD transects

##### 3.1.1. Interannual variability in properties and watermass presence

Seawater properties across the SRT undergo variability at all depths, on timescales ranging from diurnal to decadal. Distally sourced water masses, modified to varying degrees, can be identified in the SRT data, depending on oceanographic conditions, such as the competing north Atlantic gyres and position of the subpolar front. Section plots (Fig. 3A) display SRT properties, along with a presence/absence section of the main intermediate water masses per station. Winter climatologies of temperature and salinity are included in Fig. 3B.

Surface waters, especially in winter (the majority of this dataset), can be mixed down to at least 650 m (Meincke, 1986) by storm activity. These waters mostly consist of ENAW, which falls close to the Harvey line ( $\pm 0.05$  salinity; Harvey, 1982) in potential temperature–salinity ( $\Theta$ – $S$ ) space (grey line and polygon in Fig. 4A), although as ENAW advects north, modification has shifted values to the fresher side. A notable feature within these layers is the salinity core of the shelf-edge/slope component of the EBC, best seen in the climatological sections (Fig. 3B). This core, with salinity  $> 35.5$ , centres between 200 and 500 m, is approximately 12–14 km wide, positioned geographically between 15 and 14.8°W (stations 15 to 13) and appears in many of the individual years measured (Fig. 3A), albeit more diffusely over the slope.

Intermediate waters, predominantly to the east of the trough, are dominated in most years by the influence of warm and saline MOW between 700 and 1000 m. The purest/least modified form of MOW, further identified by its relatively low oxygen values (see Table 1 for properties in the RT following McGrath et al., 2012), can be seen at

various thicknesses almost every year since 2010 (Fig. 3A, fourth column, orange colour). The years of 2012, 2013, 2021 and 2022 had the strongest inflection towards MOW in  $\Theta$ – $S$  space (not shown here). The presence of the cool and fresh SAIW (Table 1) is seen directly for the years 2019 and 2021, to the middle and west of the trough respectively (Fig. 3A, column 4, blue colour), and notably is concurrent with MOW to the east. Indirectly, yet strongly, SAIW influences the water column to the west of the trough seen in  $\Theta$ – $S$  space (Fig. 4A) in many of the years examined. The winter transect of 2010 was anomalous, in that MOW type water was found to the west and east of the trough, while SAIW was present in the central trough (Fig. 3A, first row, fourth column). This was possibly due to mesoscale activity transporting MOW into western trough waters, with evidence of a large cold-core vortex, centred on station 21, in the 2010 temperature section (Fig. 3A, first row, first column).

LSW is constrained by bathymetry to recirculate around the RT (Holliday et al., 2000). At least two new pulses of LSW entered the trough, a distinctly strong pulse in 2011 and smaller but clear ingresses between 2019 and 2021 (Fig. 3A, fourth column). Water property criteria defining new LSW entering the trough, are narrow in salinity and oxygen boundary limits ( $\leq 34.92$ ,  $\geq 271$   $\mu\text{mol/kg}$ ; Table 1), while range of depths accepted has been kept wide to account for upper and lower modes of LSW (Kieke et al., 2009).

Overall, Figs. 3 and 4 demonstrate large interannual and spatial variability in properties across the transect except in deep waters below 2300 m. An example of this spatial variability can be seen in  $\Theta$ – $S$  space at intermediate depths, where the years of 2021 and 2022 are split geographically between the eastern slope stations inflecting towards MOW and the western/central stations on the fresh side of the Harvey line tending towards SAIW (Fig. 4B), as seen in the early 2000s by (2010).

##### 3.1.2. Spatial variability, averages and anomalies across trough

Further evidence of spatial variability is seen when comparing the SRT (Fig. 4C) with the mid-RT section (Fig. 4D). It is clearly evident that as upper and intermediate waters advect to the northeast, they are strongly modified and indeed homogenised from their clearer water mass signatures in the SRT to much narrower property ranges at mid-RT. This homogenisation over a relatively short distance ( $\sim 290$  km) will be through a combination of winter mixing down from surface waters, isopycnal mixing, and diapycnal mixing from mesoscale activity, including the permanent, non-stationary anticyclone centred in the mid-RT (Le Corre et al., 2019; Smilenova et al., 2020).

Specifically for intermediate waters, interannual variability can be further viewed through yearly variables (averaged across trough) that include the water masses of MOW, SAIW and ENAW (Fig. 5). Temperature between 700 and 1000 m (Fig. 5A) varies within a 1 °C range apart from the exceptionally cool 2019, while minimum and maximum values were relatively consistent around their means. The years noted earlier for defined MOW presence are warmest. Salinity typically co-varied with temperature (Fig. 5B), but with greater variation in minimum/maximum values, especially for minimums, which sat further from the means. Freshening anomalies are seen again in 2019 and also in the 2010 minimum average value, further highlighting 2010 as anomalous in its structure. Likewise, depths between density surfaces ( $\sigma_\theta$  of 27.3–27.6  $\text{kg m}^{-3}$ ; e.g. Ullgren and White, 2010) vary in thickness (and associated stability/stratification) over the years, with lighter water showing most variation, and 2019 again being anomalously shallow (Fig. 5C). Maximum, minimum and mean salinities across these threshold isopycnals also vary between years, with 2019 and 2010 showing the freshest averages at the deeper isopycnal; 27.6  $\text{kg m}^{-3}$  (Fig. 5D). It is likely that the fresher intermediate waters and ingress of SAIW seen in 2010 are reflective of expanded SPG conditions just prior to a rapid decrease seen in the monthly SPG Index which occurred from late 2009 to late 2010 (Fig. 5E; Chafik, 2019). Higher intermediate salinity averages over the following years (2011–2014; e.g. Fig. 5B–D),

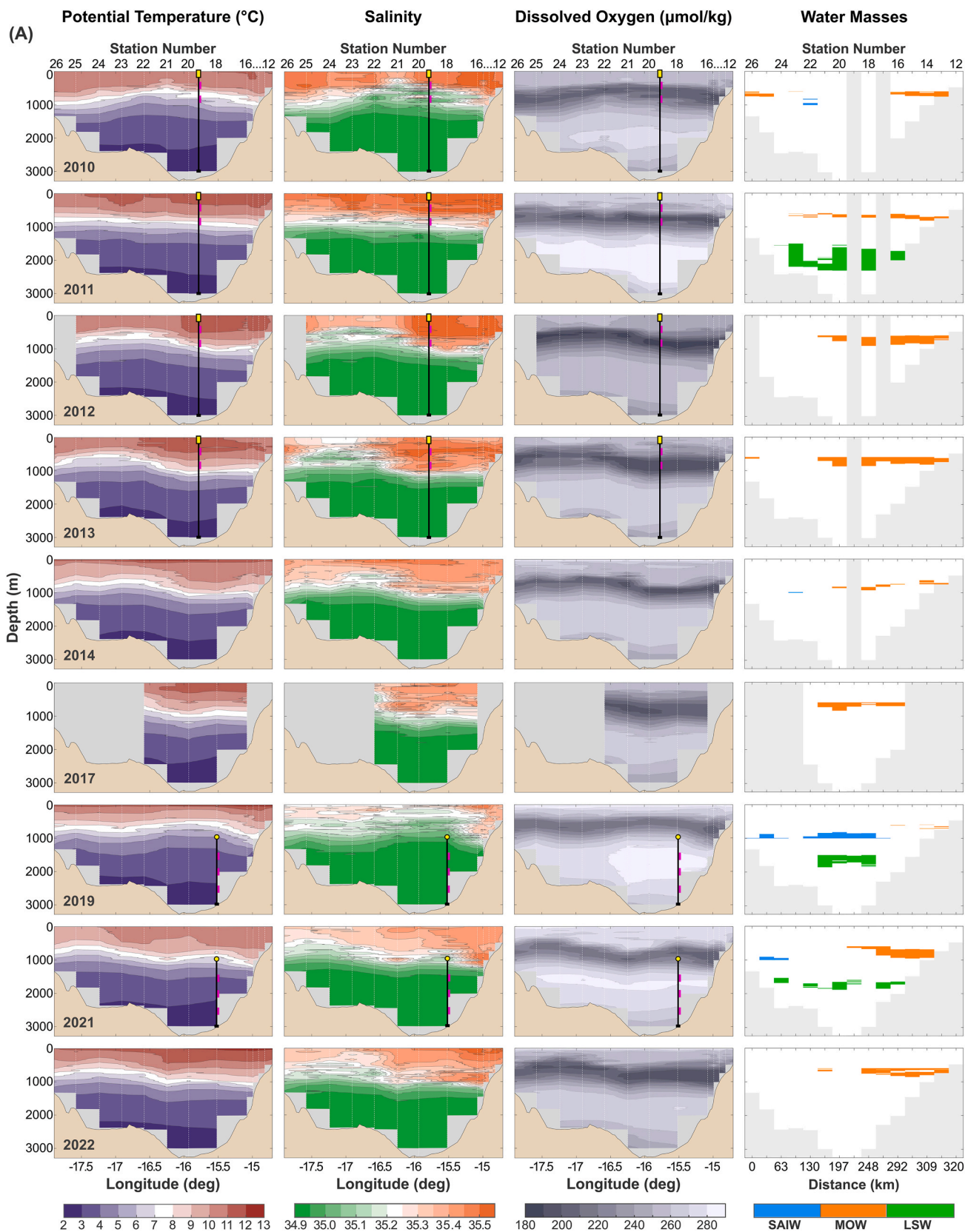


**Fig. 3A.** Section plots of temperature (first column), salinity (second column), and dissolved oxygen (third column) across the SRT for all years that obtained oxygen data. Fourth column displays the presence of specific water masses according to the parameters in Table 1. Where mooring data was coincident with a CTD transect, the position has been marked with a small mooring illustration on each section (M6 Met buoy: 2010–2013; SRT subsurface: 2019–2021) and indicated in Fig. 7A and B, later.

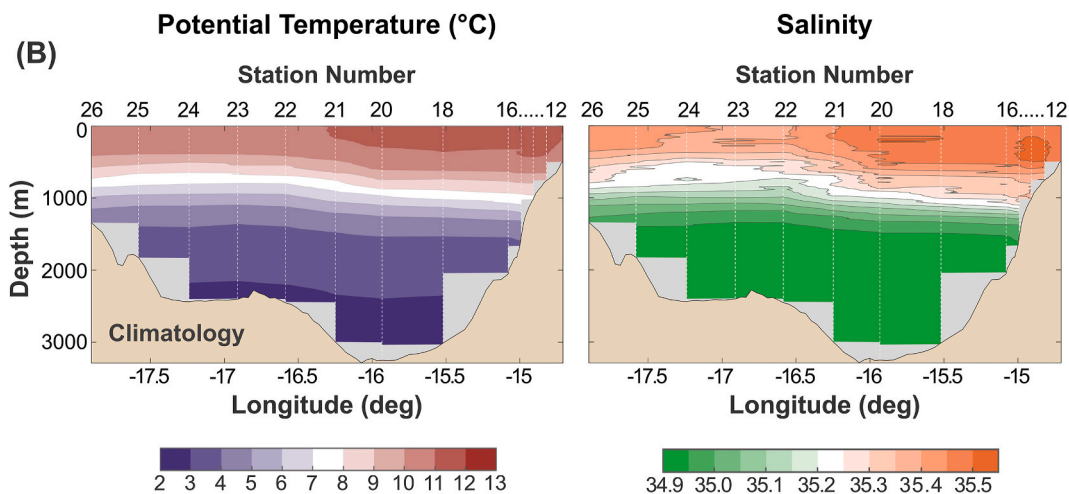


Fig. 3B. Climatology section plots for temperature and salinity, calculated from all the winter campaigns (2006–2022), are shown. Note the patch of most saline water between 200 and 500 m around 15°W, representing a salinity core of the slope current. Fig. 3A: double column, 190 mm wide (7480px) at 1000dpi.

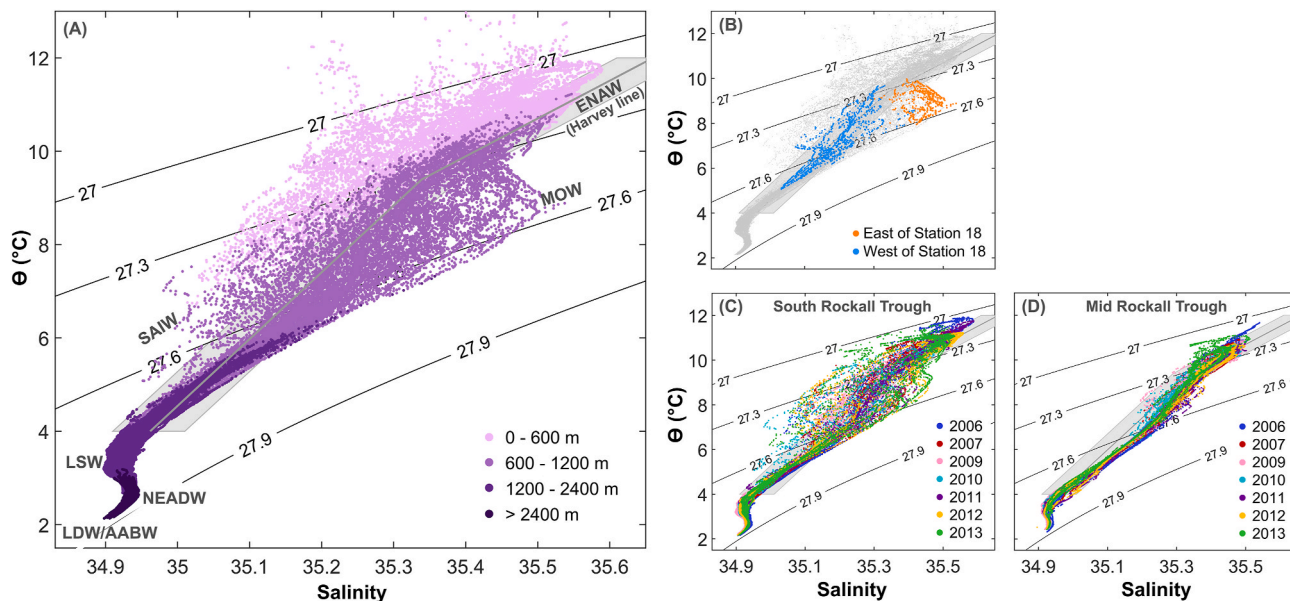


Fig. 4. Potential temperature salinity plots. All stations from all cruises across the SRT are coloured by depth bins in (A), with regions of the predominant water masses identified and labelled. Panel (B) displays intermediate water, split geographically west (blue) and east (orange) of station 18 during the years 2021 and 2022. Panels (C) and (D) illustrate the difference in water mass variability between the south and mid-Rockall Trough transects respectively, for years 2006–2013, coloured by year.

Table 1  
Criteria used to define watermass distribution for the South Rockall Trough in Figs. 3 and 4; following McGrath et al. (2012).

Watermass	Depth (m)	Temperature (°C)	Salinity	Oxygen (μmol/kg)
SAIW, Sub-Arctic Intermediate Water	700–1000	≤5.93	≤35.12	≥234
MOW, Mediterranean Overflow Water	700–1000	≥9.12	≥35.32	≤211
LSW, Labrador Sea Water	1500–2300		≤34.92	≥271

reflect negative SPGI values and indicate a more southerly ‘MOW type’ water. There is little coherence, at least visually, between these inter-annual variabilities and the NAO index, excepting in 2010 (Fig. 5E; NOAA, 2023), indicating that the region may be too dynamic for a more

defined pattern to emerge. Considering salinity along isopycnals (Figs. 5D), 2022 is uncharacteristic due to having a fresher mean value along its lighter density anomaly. The wide range between minimum and maximum salinities found each year along the selected density surfaces, indicates complex, non-uniform water mass interaction with isopycnal mixing potential within the trough at these depths.

Another method of displaying results from the SRT ocean climate dataset is by examining anomalies from the climatology over a given depth. A depth range of 250–600 m is considered important for the well-studied target fisheries species, Blue Whiting (*Micromesistius pou-tassou*) (Miesner and Payne, 2018), and is presented as temperature and salinity anomalies, spanning all stations occupied in winter across the SRT between 2006 and 2022 (Fig. 6). In general, anomalies are greater over the deeper stations (26–18, west-east; see Fig. 1C), while stations 16–12 over the slope (<2000 m bottom depth) remained closer to the climatology. 2006 was the warmest at these depths, 2021 the coldest and freshest, and the years 2009–2013 show the greatest spatial

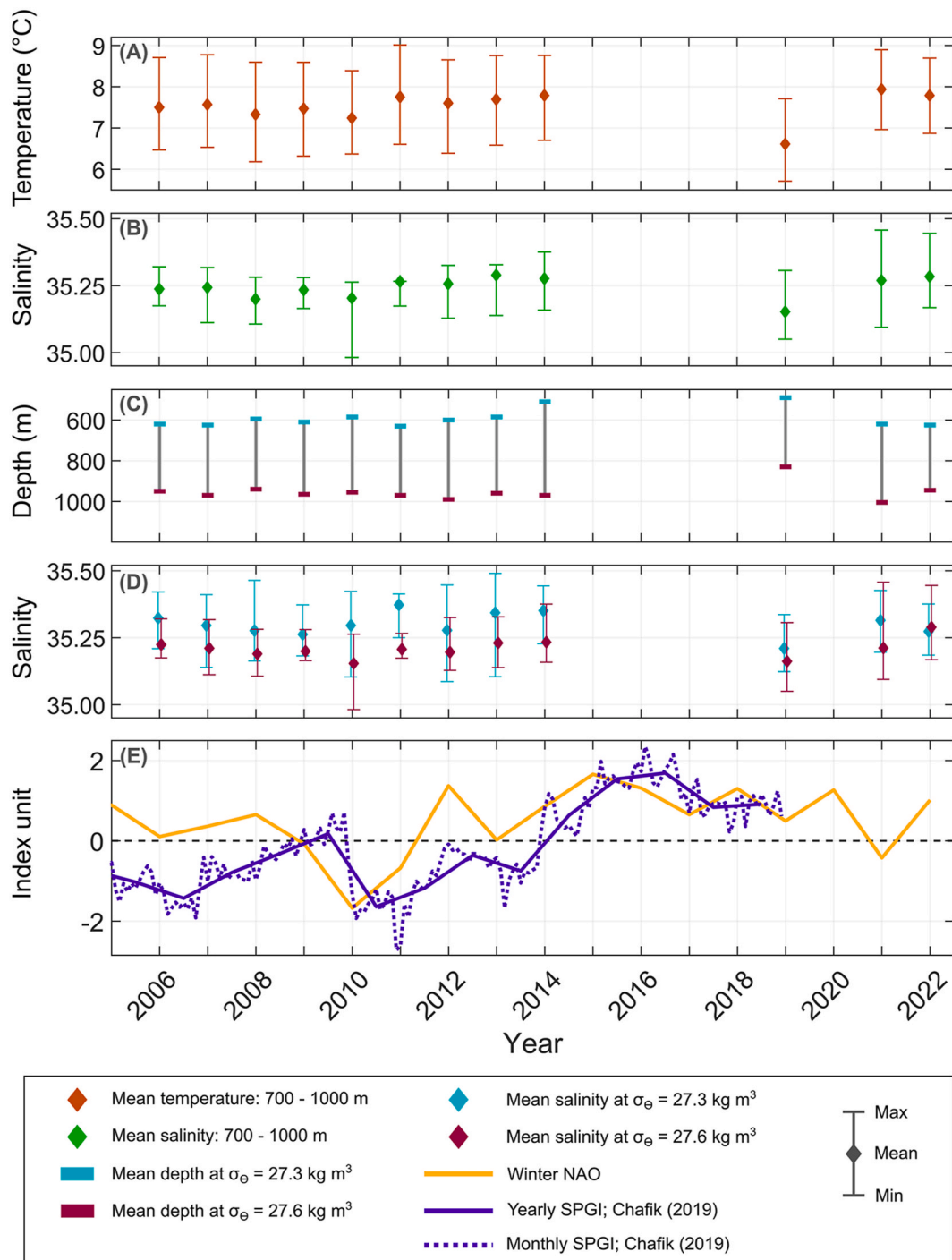


**Fig. 5.** Interannual, intermediate water column ranges and variability. Panel (A; temperature) and Panel (B; salinity) display minimums, maximums and means across trough, between 700 and 1000 m per year. Panel (C) shows averaged depths for specified isopycnals across the transect per year (as defined in the legend). Panel (D) shows average salinities across isopycnal surfaces per year, including maximum and minimum values. Panel (E) plots the winter NAO index along with monthly and yearly SPG indices, referenced in the text.

variability, with anomalies in temperature approximately concurrent with those of salinity. The anomalies presented are considerable when assessed alongside the preferred ranges of spawning Blue Whiting and larvae (salinity of 35.3–35.5 at depths of 250–600 m; [Miesner and Payne, 2018](#)).

### 3.2. Mooring data

#### 3.2.1. Presentation of mooring time-series

Subsurface fixed mooring data provide a continuous temperature and salinity time-series that is useful to track variation in water mass properties. Temperature and salinity positively co-varied at the M6 site between 2008 and 2013 and displayed a seasonal signal ([Fig. 7A and B](#)). Cooler, fresher water is more prevalent in spring or mid-year. Interannual variability was evident, with data collected in 2009 and 2010

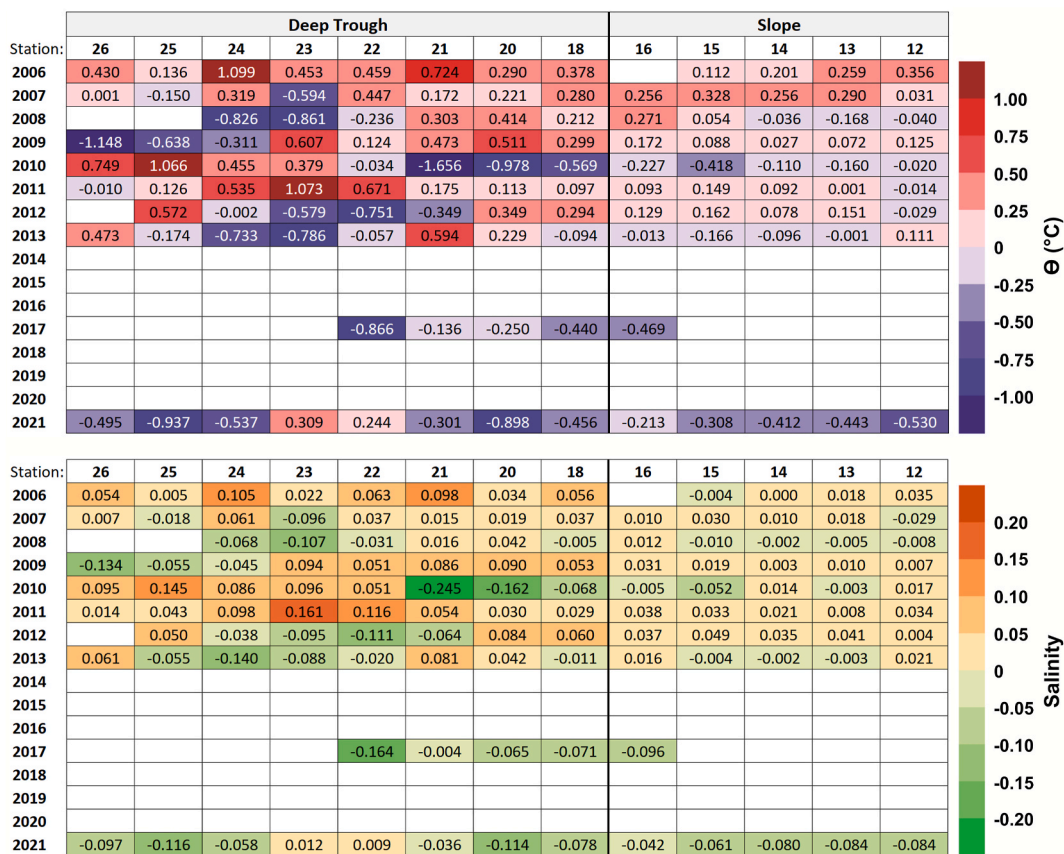


Fig. 6. Winter anomalies of temperature and salinity between 250 and 600 m at stations across the SRT. Climatology was calculated using data from all years sampled in winter.

showing bimodal impulses of colder fresher water in spring, whereas the years of 2011 and 2012 showed a more diffuse, longer period of cooler fresher conditions. All years appear warmest and most saline in winter (January, February, March).

All fixed moored data points (not interpolated) were split seasonally and are displayed in  $\Theta$ - $S$  space (Fig. 7C-F). Winter had the widest variability between  $\sigma_{\Theta}$  of 27.3 and 27.6 kg m<sup>-3</sup>, followed by autumn.

### 3.2.2. Diurnal to interannual variability in temperature and salinity

Temperature and salinity ranges at individual fixed mooring depths were gauged across a range of timescales (Table 2). Maximum daily changes were at shallower instrument depths (250–1000 m), with shifts of 1.4 °C and 1.3 °C in a single day evident in winter 2009 and summer 2010 respectively, including salinity changing by as much as 0.24 also in 2010. On occasion, the daily maximum changes in temperature and salinity were concurrent or within a couple of days of each other. A very warm and saline ‘patch’ of water can be observed passing the SRT mooring over the course of four days (25th–29th October 2018), identified as a maximum daily increase (positive sign of values in maximum difference column; Table 2) at 1200 m on the 25th and a maximum decrease at 1500 m on the 29th. This event penetrated to 2500 m in temperature data, potentially identifying very deep eddy activity. Monthly ranges were largest at shallower instrument depths in spring and summer, with temperature and salinity variations of 3.5 °C and 0.4. Deep water variability (>1200 m) was most evident in autumn and winter, with monthly changes decreasing in magnitude with depth. Yearly spread, although only marginally larger than monthly spread, is quite considerable, especially in upper/intermediate waters. Yearly shifts of up to 5 °C in temperature and 0.5 in salinity within the water column are major when considering environmental stressors on niche fisheries habitats. Highest variability across temporal scales (Table 2)

occurred at 750 m followed by 1000 m, both coincident with the intermediate water masses that compete for position in the south Rockall Trough.

## 4. Discussion

The standard hydrographic section and fixed mooring time-series presented were used to identify and monitor several watermasses in the region; interrogate features and processes, such as the eastern boundary current and remote impacts of gyre interactions; and to assess inherent variabilities. Results show the magnitude of the variability across the SRT, reflecting how dynamic the region is in general. Inter-annually, particular water masses will prevail (Fig. 3, fourth column), steered by processes which dictate the position of the North Atlantic gyre fronts, the pathways of the NAC and the strength and character of the EBC. The variability of these processes and interactions manifest as interannual fluctuations of internal water column structure seen right across the trough (Fig. 3, e.g. temperature, salinity and oxygen columns). This variability, particularly at intermediate depths, has been commonly noted (e.g. Holliday et al., 2000; Ullgren and White, 2010), for instance, where SAIW sourced water, (high nutrients and oxygen, and a low AOU) showed changes in its distribution and intensity each year (McGrath et al., 2012). Variability in the strength of intermediate water signatures was evident in this study, with large interannual variability of temperature, salinity and the depth range of density surfaces (Fig. 5; Table 2).

### 4.1. Variable conditions within the Rockall trough

#### 4.1.1. Seasonality

Seasonality will be strongest in surface mixed layers due to

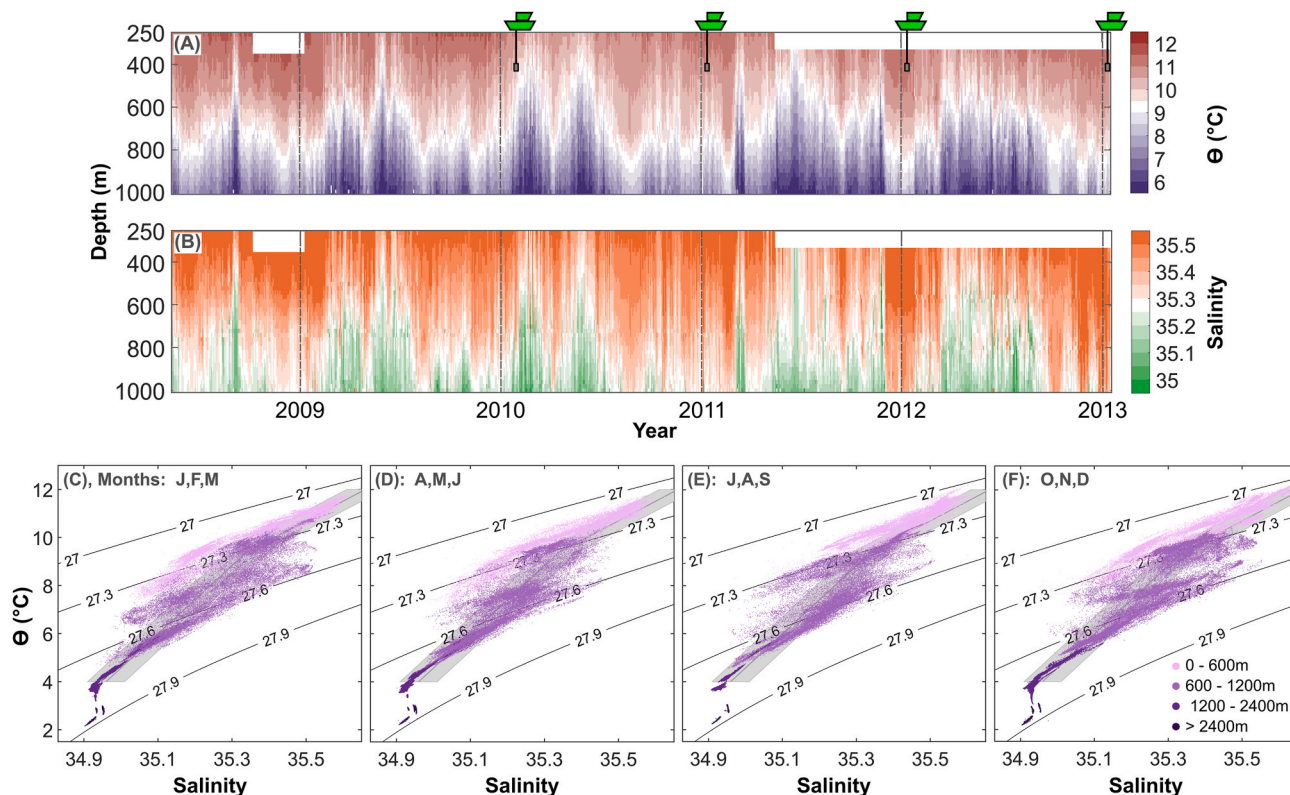


**Fig. 7.** Top panels are M6 fixed mooring time-series of temperature (A) and salinity (B). Dashed vertical lines per year are positioned on January 1st. Where mooring data is coincident with CTD transects in time, green vessel illustrations have been added to the timeseries, which match the mooring illustrations seen in Fig. 3A. The  $\Theta$ -S plots in panels (C) through (F) display all M6 and SRT subsurface data points (not interpolated), colour binned by depth and grouped seasonally (where winter is defined as J,F,M = January, February, March).

stratification caused by surface heating, where the seasonal thermocline just below this mixed layer can inhibit deeper penetration of signals. Seasonal changes were also observed throughout the intermediate water column in monthly data, where change is greatest in temperature, at 1000 m and below, in autumn and early winter (S, O, N, D, J), with salinity variation tracking temperature at most measured fixed depths (Table 2). Seasonality (and interannual variation within that seasonality), can be seen at intermediate depths through alternating cooler/fresher conditions in summer and warmer/more saline conditions in winter (Fig. 7A and B). This is further observed in  $\Theta$ -S space where the range of salinities are somewhat seasonal between  $\sigma_{\theta}$  of 27.3 and 27.6, indicating seasonally varying water mass presence or interaction (Fig. 7C-F). Intermediate water seasonality is not fully defined in the literature. While Holliday (2003) finds the warmest months (in heat content anomaly) to be in December and January (between 600 and 900 m), similar to this study, they find this cycle is not statistically significant. Large variability on a range of timescales, for example, from gyre circulation, NAO influence and shorter term mesoscale activity, can effectively mask any seasonal signals (e.g. Ullgren and White, 2010).

#### 4.1.2. Spatial heterogeneity

Intermediate water masses across the mid-RT have been homogenised through mixing, compared to the SRT. McGrath et al. (2012) found clear evidence of ENAW, with no evidence of SAIW or MOW across the mid-RT in 2009 and 2010, while Smilenova et al. (2020) found water mass fractions of up to 55% MOW, 35% SAIW (with ENAW unquantified) in 2011 (with higher MOW and lower SAIW in 2007) in the central mid-RT. This contrast highlights the complexities in both the inherent RT dynamics and in applying different methodologies (i.e. chemical analysis vs. physical mixing triangles) to investigate water masses in the region. The spatial and temporal variability shown here, when combined with the presence of mesoscale activity and winter mixing,

indicates that active modification is occurring throughout the water column, both upstream and across the SRT. This modification extends over the eastern slope, as the water column continues to mix and advect to a much more homogeneous state across the mid-RT. Homogenisation will continue through to the northern end of the central RT, where assessing or defining water masses becomes even more difficult (e.g. Fraser et al., 2022). Enhanced mixing is likely at SRT relative to these adjacent areas, due to the confluence of watermasses and of the meandering or unstable current systems of the NAC and EBC, as everything gets funneled up through the trough.

Geographically, there is a zonal split in physical properties along the outer continental margin, approximately where deeper bathymetry meets the lower slope (between stations 17 and 18,  $\sim 16.5^{\circ}$ W, depth  $\sim 3000$  m, Fig. 1C;  $\Theta$ -S space in 2021 and 2022, Fig. 4B). A spatial split has been previously noted in the SRT (e.g. McGrath et al., 2012), being described further west at  $18^{\circ}$ W (Ullgren and White, 2010). This zonal difference in water mass properties indicates a highway of warmer, more saline MOW influenced water found over the slope, at least in some years (2012, 2013, 2021 and 2022) and at certain times of the year (i.e. autumn/winter, Fig. 7). Variation in properties is large around the area of the zonal split, as seen through maximum differences from fixed mooring data across temporal scales (stations 18 and 19, Table 2). This large variability shows the mooring sites to be very dynamic over time and hence an area of enhanced mixing, where a number of water masses can transit through the eastern SRT at this location. The fact that episodes of cooler, fresher, SAIW-like water frequent the mooring site at  $16^{\circ}$ W (Fig. 7A and B) bolsters the argument for the presence of SAIW creating a barrier to the northward progression of MOW during periods of an expanded SPG (e.g. Johnson and Gruber, 2007; Lozier and Stewart, 2008; Ullgren and White, 2010).

**Table 2**

Maximum variance in potential temperature [ $\Theta$ ](°C) and salinity from fixed mooring CTD instruments measured in any given day, month, year and per deployment. To calculate these values, each individual instrument deployment analysis only considered samples within a narrow pressure band ( $\pm 10$  dbar) and passed through a 48 h filter to remove tidal influences. Date of occurrence, Month/Year and Year columns are the times when each corresponding maximum difference occurred.

Deployment	Date Range	Nominal Depth (m)	Mean Pressure (dbar)	Maximum daily variance				Maximum monthly variance				Maximum yearly/per-deployment variance			
				$\Theta$ (°C)		Salinity		$\Theta$ (°C)		Salinity		$\Theta$ (°C)		Salinity	
				Maximum difference <sup>a</sup>	Date of occurrence	Maximum difference <sup>a</sup>	Date of occurrence	Maximum difference <sup>a</sup>	Month/Year	Maximum difference <sup>a</sup>	Month/Year	Maximum difference	Year	Maximum difference	Year
M6 deployment series <sup>b</sup>	14/05/2008 to 12/01/2013	250	247, 228, 319 <sup>b</sup>	-0.67	21/11/2011	-0.14	21/11/2011	-1.92	05/2009	-0.30	06/2011	2.69	2011	0.43	2011
		750	729, 716, 775 <sup>b</sup>	-1.40	15/02/2009	-0.22	23/11/2011	-3.48	05/2009	0.42	11/2011	4.82	2011	0.53	2011
		1000	1007, 1008, 1032 <sup>b</sup>	1.29	10/06/2010	0.24	19/10/2010	2.86	09/2012	0.34	09/2012	3.62	2009	0.49	2010
SRT deployment 1	02/10/2018 to 26/05/2019	1200	1204	0.31	25/10/2018	0.04	25/10/2018	0.88	10/2018	0.12	10/2018	1.37	n/a <sup>c</sup>	0.18	n/a <sup>c</sup>
		1500	1467	-0.23	29/10/2018	-0.03	29/10/2018	0.50	10/2018	0.06	10/2018	0.72	n/a <sup>c</sup>	0.08	n/a <sup>c</sup>
		1700	1731	-0.10	07/12/2018	-0.01	5/15/2019	-0.32	12/2018	-0.01	05/2019	0.43	n/a <sup>c</sup>	0.02	n/a <sup>c</sup>
		2500	2524	0.06	29/10/2018	0.00	10/9/2018	-0.19	10/2018	0.00	11/2018	0.27	n/a <sup>c</sup>	0.01	n/a <sup>c</sup>
SRT deployment 2	26/04/2020 to 13/03/2021	1200	1183	-0.41	03/03/2021	0.07	16/01/2021	-1.10	01/2021	-0.14	03/2021	1.60	n/a <sup>c</sup>	0.21	n/a <sup>c</sup>
		1500	1448	0.20	13/08/2020	0.02	13/08/2020	-0.58	01/2021	-0.06	01/2021	0.73	n/a <sup>c</sup>	0.07	n/a <sup>c</sup>
		1700	1711	-0.11	16/01/2021	-0.01	05/05/2020	-0.33	01/2021	-0.03	10/2020	0.45	n/a <sup>c</sup>	0.03	n/a <sup>c</sup>
		2500	2503	-0.05	13/12/2020	0.00	09/09/2020	0.29	10/2020	0.01	09/2020	0.40	n/a <sup>c</sup>	0.01	n/a <sup>c</sup>

<sup>a</sup> For daily and monthly maximum differences, the sign of the value denotes direction of change, where +ve is warming/salinifying and -ve is cooling/freshening.

<sup>b</sup> The M6 deployment series consisted of three consecutive deployments, with very short (<24 h) interruptions for instrument swap out inbetween. Each deployment had slightly different depths from their nominal/target depth.

<sup>c</sup> Maximum differences here are for length of deployment, with neither of the SRT deployments lasting a full year (see Date Range column).

#### 4.1.3. Mesoscale impacts

The year 2010 was anomalous across the SRT, from upper waters down to at least lower intermediate layers. Of four years studied, McGrath et al. (2012) found a more mixed SRT in 2010 with SAIW in the mid-trough, identified with higher nutrient values, higher oxygen and lower AOU than adjacent waters either side. The temperature structure throughout (Fig. 3A, row 1, column 1) resembled a large upwelling, cold-core cyclone centred at station 21 (~16.5°W). However, on appraisal of online data products of surface currents, SSH and SST for mid-February 2010 (not shown here), there was no defined cyclonic vortex, rather a cold depressed region nestled between a large warm-core eddy to the southwest and the permanent anticyclone across the mid-RT. An oxygen minimum zone was present at MOW depths, tight against the slope (stations 14–15, Fig. 3A, row 1, column 3), but most interesting and anomalous is MOW-type water situated along the western boundary of the SRT (stations 26–25, Fig. 3A, row 1, column 4). Intermediate averages across the trough show data from the 2010 ocean climate cruise as one of the freshest and coldest years of the time-series between 700 and 1000 m (except for 2019), with the lowest salinity minimums, maximums and means along the 27.6 isopycnal (Fig. 5A, B and D). Regardless of the impact of a large eddy in 2010, all water mass analyses from ship-based and fixed mooring CTDs here are conducted under a constant backdrop of mesoscale activity, as eddies are spun off the NAC, with some directly entering the RT (e.g. Wade et al., 1997; Moritz et al., 2021). Although these eddies provide a transport mechanism that is likely responsible for the MOW-type water found to the west in 2010, they also blur any clear signal of water mass interaction and other mixing mechanisms at the mouth of the RT. In doing so, these vortices prove themselves as a major driver of mixing as they pass through, in places interacting with topography, quite noticeable along the path of the slope current (e.g. Smilenova et al., 2020).

#### 4.1.4. The mid-2010s freshening event

In 2016 the northeast North Atlantic region, including the SRT, experienced an unprecedented freshening event in upper waters, caused by changes in ocean circulation, likely driven by changes in the wind stress field (e.g. Holliday et al., 2020), or reduced heat loss from the Labrador Sea surface (Fox et al., 2022). While 2016 and adjacent years were not captured in our time-series, a limited number of stations were occupied in 2017 that displayed anomalously fresh and cool water (e.g. between 250 and 600 m; Fig. 6). The summer of 2019 remained very fresh and cool, with anomalous values between 700 and 1000 m and including a narrower (more stable), fresher band between density surfaces of 27.3 and 27.6 kg m<sup>-3</sup> (Fig. 5A–D). This was a continuation of cool fresh conditions from the preceding years, similar to that measured in northern waters of the RT, along the Ellett Line; displayed as anomalies from the mean in the ICES Report on Ocean Climate (see Fig. 2.2 and Table 2.1 at location #16 in Gonzalez-Pola et al., 2022). Although the lack of yearly data prevents making a direct link between 2016 and 2019, it is nonetheless interesting to note the anomaly seen in 2019 extends at least as deep as the 27.6 isopycnal, being deeper than 800 m that year.

#### 4.2. The eastern boundary current system

A salinity core associated with the EBC is clearly evident in climatological sections, extending between stations 15 and 13 (15–14.8°W, respectively; 12–14 km wide) and between 200 and 500 m (Fig. 3B). In any given year, depending on the season and forcing conditions, such as mesoscale activity or deep winter mixing, the salinity core of the slope current may be more diffuse across the trough or indeed non-existent. The literature is somewhat unresolved on the proximity, steadiness and forcing mechanisms of the EBC at this location. Just to the north at ~54.5°N the slope current is persistently poleward and stronger with steeper slope gradients (White and Bowyer, 1997). The slope current is further strengthened off the Hebrides to the north (e.g. Booth and Ellett,

1983; Souza et al., 2001) being strongest in spring (Fraser et al., 2022), while following a SOMA (Sept, Oct, Mar, Apr) seasonal pattern south of our area (e.g. Pingree et al., 1999; Huthnance et al., 2001). A deep (>3000 m) along slope bottom boundary current, arguably a constituent of the EBC system, is described at the same latitudes as this study, with mean flows of 2.5 cm s<sup>-1</sup> and (as commonly observed in boundary current systems), displays large variability in flow strength and direction, in this case mostly driven by internal tidal energy (Thorpe, 1987).

Additional to the well described poleward flow of the EBC over the slope (west of the Porcupine Bank), there appears to be a shallow “branch” of that flow navigating over the deepest part of the shelf (~400 m seafloor depth), east of the Porcupine Bank (~200 m seafloor depth) and west of the Irish shelf along the 53°N line (~200 m seafloor depth). This relatively warm, saline intrusion over the shelf is a topographically steered continuation of cyclonic flow within the Porcupine Sea Bight, where deeper components of flow are constrained to recirculate (McMahon et al., 1995; White and Bowyer, 1997). This feature is best visualised as a winter anomaly of Absolute Dynamic Topography (ADT) derived geostrophic currents (Fig. 6 from Xu et al., 2015). An anticyclonic rotation around the Porcupine Bank exists at slope current depths <400 m (Mohn et al., 2002), that may impede, counteract or push east the through-flow of any Porcupine Sea Bight derived shelf edge current. An initial appraisal of the ocean climate cruise data in our study suggests that indeed there is northward flow, at least in winter, coupled with a saline wedge extending north over the deepest part of the western Irish shelf. Future work aims to incorporate ADT analysis along with other methods (e.g. deploying fixed depth ADCPs) to further investigate this potential pathway.

#### 4.3. Labrador Sea Water presence and pulses

Strong ‘pulses’ or spatial presence of LSW (defined for the RT in Table 1) were present in 2011, 2019 and 2021 (Fig. 3A, column 4). The largest pulse was in 2011, spanning the depths of 1600–2200 m at stations in the central SRT; enveloping the expected depths of both upper and deep LSW. The pathways of source LSW to the RT are complex (e.g. Fig. 1 from Rhein et al., 2017) and will vary over time, at least partly due to the same drivers that alter the character and position of the North Atlantic gyre systems (Kieke et al., 2009). However, assuming a transit lag of approximately a decade from source formation in the Labrador Sea (Yashayaev et al., 2007), the strong signal of LSW in 2011 is consistent with strong formation conditions in 2000 (LSW<sub>2000</sub> class; see top right panel of Fig. 3 in Yashayaev et al., 2007). Likewise, the 2019 pulse could have originated from the LSW<sub>2008</sub> class (Yashayaev and Loder, 2017), while the 2021 pulse may indicate prolonged arrival or residence of water from the same event, having disappeared by 2022.

#### 4.4. Implications for marine living resources

Detailed research on understanding relationships between the physical oceanographic/environmental conditions and the resulting influences on regional marine ecosystems, has been ongoing for years, yet remains inconclusive. Blue whiting *Micromesistius poutassou*, is an example exploited fish species, with spawning grounds situated in the wider RT (~45–64°N, ~0–20°W) between 250 and 600 m, where its ‘niche’ habitat for spawning, including where the majority of adults and larvae are found, exists between a narrow salinity range of 35.3–35.5 (Miesner and Payne, 2018, and references within). Fishing activity is largely dependent on spawning with the majority of catches taking place west of the islands of Britain and Ireland during and just post the spawning season (NEAFC, 2013). Spawning distributions vary inter-annually, and are strongly related to physical conditions dictated by the expansion/contraction of the SPG, where cold fresh ‘SAIW’ conditions limit spawning to the eastern shelf edge of the RT and warmer ‘MOW/ENAW’ conditions allow a wider distribution further west beyond the trough (Miesner and Payne, 2018). Miesner et al. (2022)

demonstrated that retrospective forecasts of temperature and salinity using the dynamic Earth System Models (ESM) could be used successfully to predict suitable spawning habitats for blue whiting during peak spawning months (late March – early April). On a decadal scale, climate prediction models have also been used to model potential fish habitat and distribution shifts in three marine fish species in the northeast Atlantic (Atlantic mackerel (*Scomber scombrus*), Bluefin tuna (*Thunnus thynnus*) and Blue Whiting) (Payne et al., 2022). The above studies highlight the potential benefits of incorporating oceanographic data into species distribution models to aid in fisheries management. However, these models may not capture the complexity of oceanographic conditions that drive availability of suitable habitat conditions of fish species. This study has demonstrated that anomalies from the winter climatology 2006–2021 at expected blue whiting spawning depths (Fig. 6) show very large interannual and zonal changes within the context of a favoured niche (0.2 range in salinity). Blue whiting spawning occurs primarily from March–May and although the current study examines oceanographic conditions over the winter pre-spawning period it still gives an important insight into the complexities of the marine environment. Pre-spawning conditions have been shown to effect blue whiting populations with a previous study on a population in the NW Mediterranean linking the recruitment success of blue whiting to preceding winter temperatures with longer cold periods (~13 °C) leading to improved recruitment (Mir-Arguimbau et al., 2022). Additionally, large daily and monthly swings in Eulerian salinity measurements (Table 2) highlight the complex distribution of the ideal habitat conditions during both SPG modes (expansion or contraction). Therefore, it is essential that any species distribution model, incorporating modelled physical parameters, is underpinned by observational oceanographic data across a number of platforms, and unrestricted by the limitations of any one platform type. Oceanographers from multiple fields need to continue building knowledge on biophysical interactions in the RT region, with work planned by the authors to further investigate the potential use of multiple existing oceanographic datasets and data products along with key fishery species datasets.

#### 4.5. Concluding remarks

In conclusion, the datasets presented here enhance our knowledge of water mass interaction and variability across the south Rockall Trough. Continuation of the time-series will add longevity to analyses and provide further insight into norms and extremes in properties and processes influencing the RT. Such time-series can add context to other studies in the region, such as ocean-shelf exchange (e.g. Huthnance et al., 2022), or shallowing aragonite saturation zones (Büscher et al., 2023). Understanding and monitoring regional and wider-scale oceanographic processes and drivers is ever more important in response to global, anthropogenically forced earth system change. Listed below are some of our key findings:

- Water mass presence, extent and proportionality in the SRT are variable over a range of timescales, driven by remote large-scale and local processes
- *In-situ* variability at fixed sites can be considerable (e.g. daily differences: 1.4 °C and 0.22; monthly: 3.48 °C and 0.42; annually: 4.82 °C and 0.53, in temperature and salinity respectively at 750 m)
- Mesoscale activity, along with other mixing mechanisms, modify the water column, intensify water mass interaction and homogenise properties during poleward advection; very evident when comparing water structure and properties between SRT and mid-RT
- 2010 was the most anomalous year in respect to water column structure, with MOW water found on both the western and eastern flanks, and SAIW at central stations of the SRT
- There is a defined high salinity core, associated with the Eastern Boundary Current, apparent in climatological sections between 200

and 500 m, 12–14 km wide, positioned geographically between 15 and 14.8°W

- Two distinct pulses of LSW derived water are found at SRT (2011 and 2019–2021), relating to documented formation events
- Variability across timescales is quite considerable in the context of biological species niche habitat conditions. Additional research on the consequences of daily/monthly variability in observed oceanographic data on spatial distribution modelling of fish species is needed

#### CRediT authorship contribution statement

**Eoghan Daly:** Conceptualization, Data curation, Formal analysis, Investigation, Methodology, Validation, Visualization, Writing – original draft, Writing – review & editing. **Glenn Nolan:** Conceptualization, Formal analysis, Methodology, Writing – review & editing, Supervision. **Alan Berry:** Data curation, Investigation. **Janina V. Büscher:** Data curation, Investigation. **Rachel R. Cave:** Data curation, Investigation. **Levke Caesar:** Conceptualization, Data curation, Investigation. **Margot Cronin:** Data curation, Investigation. **Sheena Fennell:** Data curation, Investigation. **Kieran Lyons:** Data curation, Investigation. **Aedín McAleer:** Data curation, Investigation. **Gerard D. McCarthy:** Conceptualization, Formal analysis, Investigation, Writing – review & editing. **Evin McGovern:** Data curation, Investigation. **Joseph V. McGovern:** Formal analysis, Investigation, Methodology, Visualization. **Triona McGrath:** Data curation, Investigation. **Garvan O'Donnell:** Data curation, Investigation. **Diego Pereiro:** Data curation, Investigation, Methodology, Visualization. **Rob Thomas:** Data curation, Formal analysis, Investigation, Methodology. **Louise Vaughan:** Data curation, Investigation, Writing – original draft, Writing – review & editing. **Martin White:** Conceptualization, Data curation, Formal analysis, Writing – review & editing. **Caroline Cusack:** Conceptualization, Supervision, Writing – review & editing.

#### Declaration of competing interest

The authors declare that they have no known competing financial interests or personal relationships that could have appeared to influence the work reported in this paper.

#### Data availability

Some data is available online, some through data request. For details please see Data Availability Statement as part of main manuscript.

#### Acknowledgements

Scientific surveys were funded under the Marine Institute's Marine Research Programme by the Irish Government. The authors thank the Working Group on Ocean Hydrography (WGOH) of the International Council for the Exploration of the Sea (ICES) for facilitating this research. We are very grateful for the long-standing dedication, skill, tenacity and enthusiasm of the crew and officers of the Irish research vessels, especially in the face of adverse North Atlantic sea conditions. We also gratefully acknowledge the vessel support received from the Marine Institute RV-Ops team and everyone else who has helped over the years.

#### References

- Arhan, M., 1990. The North Atlantic current and subarctic intermediate water. *J. Mar. Res.* 48, 109–144.
- Arhan, M., Colin De Verdière, A., Mémery, L., 1994. The eastern boundary of the subtropical North Atlantic. *J. Phys. Oceanogr.* 24, 1295–1316.
- Arhan, M., King, B., 1995. Lateral mixing of the mediterranean water in the eastern North Atlantic. *J. Mar. Res.* 53, 865–895. <https://doi.org/10.1357/0022240953212990>.

- Aznar, R., Sotillo, M.G., Cailleau, S., Lorente, P., Levier, B., Amo-Baladrón, A., Reffray, G., Álvarez-Fanjul, E., 2016. Strengths and weaknesses of the CMEMS forecasted and reanalyzed solutions for the Iberia–Biscay–Ireland (IBI) waters. *J. Mar. Syst.* 159, 1–14. <https://doi.org/10.1016/j.jmarsys.2016.02.007>.
- Belkin, I.M., Levitus, S., 1996. Temporal variability of the subarctic front near the charlie-gibbs fracture zone. *J. Geophys. Res.: Oceans* 101, 28317–28324. <https://doi.org/10.1029/96JC02794>.
- Booth, D.A., Ellett, D.J., 1983. The Scottish continental slope current. *Continent. Shelf Res.* 2, 127–146. [https://doi.org/10.1016/0278-4343\(83\)90012-2](https://doi.org/10.1016/0278-4343(83)90012-2).
- Bower, A.S., Le Cann, B., Rossby, T., Zenk, W., Gould, J., Speer, K., Richardson, P.L., Prater, M.D., Zhang, H.-M., 2002. Directly measured mid-depth circulation in the northeastern North Atlantic Ocean. *Nature* 419, 603–607. <https://doi.org/10.1038/nature01078>.
- Büscher, J.V., Cave, R.R., O'Donnell, G., Cronin, M., McGovern, E., 2023. Ocean chemistry. In: Nolan, G., Cusack, C., Fitzhenry, D. (Eds.), *Irish Ocean Climate & Ecosystem Status Report*. Marine Institute, Galway, Ireland, pp. 36–59.
- Caesar, L., McCarthy, G.D., Thornalley, D.J.R., Cahill, N., Rahmstorf, S., 2021. Current atlantic meridional overturning circulation weakest in last millennium. *Nat. Geosci.* 14, 118–120. <https://doi.org/10.1038/s41561-021-00699-z>.
- Chafik, L., 2019. North Atlantic subpolar gyre index. Database Version 3. Bolin Centre Database. <https://doi.org/10.17043/chafik-2019-gyre-3>.
- Dickson, R., Lazier, J., Meincke, J., Rhines, P., Swift, J., 1996. Long-term coordinated changes in the convective activity of the North Atlantic. *Prog. Oceanogr.* 38, 241–295. [https://doi.org/10.1016/S0079-6611\(97\)00002-5](https://doi.org/10.1016/S0079-6611(97)00002-5).
- Ellett, D.J., Edwards, A., Bowers, R., 1986. The hydrography of the Rockall Channel—an overview. *Proc. Roy. Soc. Edinb. B Biol. Sci.* 88, 61–81. <https://doi.org/10.1017/S0269727000004474>.
- Ellett, D.J., Martin, J.H.A., 1973. The physical and chemical oceanography of the Rockall channel. *Deep Sea Res. Oceanogr. Abstr.* 20, 585–625. [https://doi.org/10.1016/0011-7471\(73\)90030-2](https://doi.org/10.1016/0011-7471(73)90030-2).
- Fox, A.D., Handmann, P., Schmidt, C., Fraser, N., Rühls, S., Sanchez-Franks, A., Martin, T., Oltmanns, M., Johnson, C., Rath, W., Holliday, N.P., Biastoch, A., Cunningham, S.A., Yashayaev, I., 2022. Exceptional freshening and cooling in the eastern subpolar North Atlantic caused by reduced Labrador Sea surface heat loss. *Ocean Sci.* 18, 1507–1533. <https://doi.org/10.5194/os-18-1507-2022>.
- Fraser, N.J., Cunningham, S.A., Drysdale, L.A., Inall, M.E., Johnson, C., Jones, S.C., Burmeister, K., Fox, A.D., Dumont, E., Porter, M., 2022. North atlantic current and European slope current circulation in the Rockall Trough observed using moorings and gliders. *J. Geophys. Res.: Oceans* e2022JC019291. <https://doi.org/10.1029/2022JC019291>.
- Gonzalez-Pola, C., Larsen, K.M.H., Fratantoni, P., Beszczynska-Möller, A., 2022. ICES Report on ocean climate 2020 (report). In: ICES Cooperative Research Reports (CRR). <https://doi.org/10.17895/ices.pub.19248602.v2>.
- Häkkinen, S., Rhines, P.B., Worthen, D.L., 2011. Warm and saline events embedded in the meridional circulation of the northern North Atlantic. *J. Geophys. Res.: Oceans* 116. <https://doi.org/10.1029/2010JC006275>.
- Harvey, J., 1982.  $\theta$ -S relationships and water masses in the eastern North Atlantic. *Deep Sea Research Part A. Oceanographic Research Papers* 29, 1021–1033. [https://doi.org/10.1016/0198-0149\(82\)90025-5](https://doi.org/10.1016/0198-0149(82)90025-5).
- Harvey, J., Arhan, M., 1988. The water masses of the central North Atlantic in 1983–84. *J. Phys. Oceanogr.* 18, 1855–1875. [https://doi.org/10.1175/1520-0485\(1988\)018<1855:TWMOTC>2.0.CO;2](https://doi.org/10.1175/1520-0485(1988)018<1855:TWMOTC>2.0.CO;2).
- Hátún, H., Lohmann, K., Matei, D., Jungclauss, J.H., Pacariz, S., Bersch, M., Gislason, A., Ólafsson, J., Reid, P., 2016. An inflated subpolar gyre blows life toward the northeastern Atlantic. *Prog. Oceanogr.* 147, 49–66.
- Hátún, H., Sando, A.B., Drange, H., Hansen, B., Valdimarsson, H., 2005. Influence of the atlantic subpolar gyre on the thermohaline circulation. *Science* 309, 1841–1844. <https://doi.org/10.1126/science.1114777>.
- Holliday, N.P., 2003. Air-sea interaction and circulation changes in the northeast Atlantic. *J. Geophys. Res.: Oceans* 108. <https://doi.org/10.1029/2002JC001344>.
- Holliday, N.P., Bersch, M., Berx, B., Chafik, L., Cunningham, S., Florindo-López, C., Hátún, H., Johns, W., Josey, S.A., Larsen, K.M.H., Mulet, S., Oltmanns, M., Reverdin, G., Rossby, T., Thiery, V., Valdimarsson, H., Yashayaev, I., 2020. Ocean circulation causes the largest freshening event for 120 years in eastern subpolar North Atlantic. *Nat. Commun.* 11, 585. <https://doi.org/10.1038/s41467-020-14474-y>.
- Holliday, N.P., Cunningham, S.A., 2013. The extended Ellett line: discoveries from 65 Years of marine observations west of the UK. *Oceanography* 26, 156–163.
- Holliday, N.P., Cunningham, S.A., Johnson, C., Gary, S.F., Griffiths, C., Read, J.F., Sherwin, T., 2015. Multidecadal variability of potential temperature, salinity, and transport in the eastern subpolar North Atlantic. *J. Geophys. Res.: Oceans* 120, 5945–5967. <https://doi.org/10.1002/2015JC010762>.
- Holliday, P., Pollard, R.T., Read, J.F., Leach, H., 2000. Water mass properties and fluxes in the Rockall Trough, 1975–1998. *Deep Sea Res. Oceanogr. Res. Pap.* 47, 1303–1332. [https://doi.org/10.1016/S0967-0637\(99\)00109-0](https://doi.org/10.1016/S0967-0637(99)00109-0).
- Hurrell, J.W., 1995. Decadal trends in the North Atlantic oscillation: regional temperatures and precipitation. *Science* 269, 676–679. <https://doi.org/10.1126/science.269.5224.676>.
- Huthnance, J.M., 1984. Slope currents and “JEBAR”. *J. Phys. Oceanogr.* 14, 795–810. [https://doi.org/10.1175/1520-0485\(1984\)014<0795:SCA>2.0.CO;2](https://doi.org/10.1175/1520-0485(1984)014<0795:SCA>2.0.CO;2).
- Huthnance, J.M., Coelho, H., Griffiths, C.R., Knight, P.J., Rees, A.P., Sinha, B., Vangriesheim, A., White, M., Chatwin, P.G., 2001. Physical structures, advection and mixing in the region of Goban spur. *Deep Sea Res. Part II Top. Stud. Oceanogr.* 48, 2979–3021. [https://doi.org/10.1016/S0967-0645\(01\)00030-3](https://doi.org/10.1016/S0967-0645(01)00030-3).
- Huthnance, J.M., Hopkins, J., Berx, B., Dale, A., Holt, J., Hosegood, P., Inall, M., Jones, S., Loveday, B.R., Miller, P.I., Polton, J., Porter, M., Spingys, C., 2022. Ocean shelf exchange, NW European shelf seas: measurements, estimates and comparisons. *Prog. Oceanogr.* 202, 102760. <https://doi.org/10.1016/j.pocean.2022.102760>.
- Iorga, M.C., Lozier, M.S., 1999. Signatures of the Mediterranean outflow from a North Atlantic climatology: 2. Diagnostic velocity fields. *J. Geophys. Res.: Oceans* 104, 26011–26029. <https://doi.org/10.1029/1999JC900204>.
- Johnson, C., Gruber, N., 2007. Decadal water mass variations along 20°W in the northeastern atlantic ocean. *Progress in Oceanography, Observing and Modelling Ocean Heat and Freshwater Budgets and Transports* 73, 277–295. <https://doi.org/10.1016/j.pocean.2006.03.022>.
- Johnson, C., Inall, M., Häkkinen, S., 2013. Declining nutrient concentrations in the northeast Atlantic as a result of a weakening Subpolar Gyre. *Deep Sea Res. Oceanogr. Res. Pap.* 82, 95–107.
- Johnson, C., Sherwin, T., Smythe-Wright, D., Shimmield, T., Turrell, W., 2010. Wyville Thomson Ridge overflow water: spatial and temporal distribution in the Rockall Trough. *Deep Sea Res. Oceanogr. Res. Pap.* 57, 1153–1162. <https://doi.org/10.1016/j.dsr.2010.07.006>.
- Jones, S.C., Fraser, N.J., Cunningham, S.A., Fox, A.D., Inall, M.E., 2023. Observation-based estimates of volume, heat, and freshwater exchanges between the subpolar North Atlantic interior, its boundary currents, and the atmosphere. *Ocean Sci.* 19, 169–192. <https://doi.org/10.5194/os-19-169-2023>.
- Kieke, D., Klein, B., Stramma, L., Rhein, M., Koltermann, K.P., 2009. Variability and propagation of Labrador Sea Water in the southern subpolar North Atlantic. *Deep Sea Res. Oceanogr. Res. Pap.* 56, 1656–1674. <https://doi.org/10.1016/j.dsr.2009.05.010>.
- Le Corre, M., Gula, J., Smilenova, A., Houpert, L., 2019. On the Dynamics of a Deep Quasi-Permanent Anticyclonic Eddy in the Rockall Trough, vol. 12. *Association Française de Mécanique, Brest, France*.
- Lozier, M.S., Stewart, N.M., 2008. On the temporally varying northward penetration of mediterranean overflow water and eastward penetration of Labrador Sea Water. *J. Phys. Oceanogr.* 38, 2097–2103. <https://doi.org/10.1175/2008JPO3908.1>.
- Marshall, J., Johnson, H., Goodman, J., 2001. A study of the interaction of the North Atlantic oscillation with ocean circulation. *J. Clim.* 14, 1399–1421. [https://doi.org/10.1175/1520-0442\(2001\)014<1399:ASOTIO>2.0.CO;2](https://doi.org/10.1175/1520-0442(2001)014<1399:ASOTIO>2.0.CO;2).
- Mauritzen, C., Morel, Y., Paillet, J., 2001. On the influence of mediterranean water on the central waters of the North Atlantic ocean. *Deep Sea Res. Oceanogr. Res. Pap.* 48, 347–381. [https://doi.org/10.1016/S0967-0637\(00\)00043-1](https://doi.org/10.1016/S0967-0637(00)00043-1).
- McCarthy, G.D., Joyce, T.M., Josey, S.A., 2018. Gulf stream variability in the context of quasi-decadal and multidecadal atlantic climate variability. *Geophys. Res. Lett.* 45 (11) <https://doi.org/10.1029/2018GL079336>, 257–11,264.
- McCartney, M.S., 1992. Recirculating components to the deep boundary current of the northern North Atlantic. *Prog. Oceanogr.* 29, 283–383. [https://doi.org/10.1016/0079-6611\(92\)90006-L](https://doi.org/10.1016/0079-6611(92)90006-L).
- McCartney, M.S., Mauritzen, C., 2001. On the origin of the warm inflow to the Nordic Seas. *Prog. Oceanogr.* 51, 125–214. [https://doi.org/10.1016/S0079-6611\(01\)00084-2](https://doi.org/10.1016/S0079-6611(01)00084-2).
- McGrath, T., Nolan, G., McGovern, E., 2012. Chemical characteristics of water masses in the Rockall Trough. *Deep Sea Res. Oceanogr. Res. Pap.* 61, 57–73. <https://doi.org/10.1016/j.dsr.2011.11.007>.
- McMahon, T., Raine, R., Titov, O., Boychuk, S., 1995. Some oceanographic features of northeastern Atlantic waters west of Ireland. *ICES (Int. Coun. Explor. Sea) J. Mar. Sci.* 52, 221–232. [https://doi.org/10.1016/1054-3139\(95\)80037-9](https://doi.org/10.1016/1054-3139(95)80037-9).
- Meincke, J., 1986. Convection in the oceanic waters west of Britain. *Proc. Roy. Soc. Edinb. B Biol. Sci.* 88, 127–139. <https://doi.org/10.1017/S0269727000004504>.
- Miesner, A.K., Payne, M.R., 2018. Oceanographic variability shapes the spawning distribution of blue whiting (*Micromesistius poutassou*). *Fish. Oceanogr.* 27, 623–638. <https://doi.org/10.1111/fg.12382>.
- Miesner, A.K., Brune, S., Pieper, P., Koul, V., Baehr, J., Schrum, C., 2022. Exploring the potential of forecasting fish distributions in the north east atlantic with a dynamic earth system model, exemplified by the suitable spawning habitat of blue whiting. *Front. Mar. Sci.* 8 <https://doi.org/10.3389/fmars.2021.777427>.
- Mir-Arguimbau, J., Flexas, M.M., Salat, J., Martín, P., Balcells, M., Raventós, N., Sabatés, A., 2022. Severe winter conditions improve recruitment success of blue whiting (*Micromesistius poutassou*), a temperate water fish species, in the NW Mediterranean Sea. *Prog. Oceanogr.* 205, 102818. <https://doi.org/10.1016/j.pocean.2022.102818>.
- Mohn, C., Bartsch, J., Meincke, J., 2002. Observations of the mass and flow field at Porcupine Bank. *ICES J. Mar. Sci.* 59, 380–392.
- Moritz, M., Jochumsen, K., Kieke, D., Klein, B., Klein, H., Köllner, M., Rhein, M., 2021. Volume transport time series and variability of the North Atlantic eastern boundary current at goban spur. *J. Geophys. Res.: Oceans* 126, e2021JC017393. <https://doi.org/10.1029/2021JC017393>.
- NEAFC, 2013. In: *Report from the NEAFC Working Group on Collating Information on the Distribution of All Life Stages of Blue Whiting in the North-East Atlantic and the Distribution of Catches from the Stock*, London, 26 – 28 November 2013. NEAFC, London.
- Needler, G.T., Heath, R.A., 1975. Diffusion coefficients calculated from the mediterranean salinity anomaly in the North Atlantic ocean. *J. Phys. Oceanogr.* 5, 173–182. [https://doi.org/10.1175/1520-0485\(1975\)005<0173:DCCFTM>2.0.CO;2](https://doi.org/10.1175/1520-0485(1975)005<0173:DCCFTM>2.0.CO;2).
- New, A.L., Barnard, S., Herrmann, P., Molines, J.-M., 2001. On the origin and pathway of the saline inflow to the Nordic Seas: insights from models. *Progress in Oceanography, Dynamics of the North Atlantic Circulation: Simulation and Assimilation with High-Resolution Models (DYNAMO)* 48, 255–287. [https://doi.org/10.1016/S0079-6611\(01\)00007-6](https://doi.org/10.1016/S0079-6611(01)00007-6).

- New, A.L., Smythe-Wright, D., 2001. Aspects of the circulation in the Rockall Trough. Continental shelf research. The Marine Environment of the North East Atlantic Margin 21, 777–810. [https://doi.org/10.1016/S0278-4343\(00\)00113-8](https://doi.org/10.1016/S0278-4343(00)00113-8).
- NOAA, 2023. Climate Prediction Center - North Atlantic Oscillation (NAO) [WWW Document]. <https://www.cpc.ncep.noaa.gov/data/teledoc/nao.shtml>. (Accessed 31 January 2023).
- Nowitzki, H., Rhein, M., Roessler, A., Kieke, D., Mertens, C., 2021. Trends and transport variability of the circulation in the subpolar Eastern North Atlantic. J. Geophys. Res.: Oceans 126, e2020JC016693. <https://doi.org/10.1029/2020JC016693>.
- Orvik, K.A., Skagseth, Ø., 2003. The impact of the wind stress curl in the North Atlantic on the Atlantic inflow to the Norwegian Sea toward the Arctic. Geophys. Res. Lett. 30 <https://doi.org/10.1029/2003GL017932>.
- Payne, M.R., Danabasoglu, G., Keenlyside, N., Matei, D., Miesner, A.K., Yang, S., Yeager, S.G., 2022. Skilful decadal-scale prediction of fish habitat and distribution shifts. Nat. Commun. 13, 2660. <https://doi.org/10.1038/s41467-022-30280-0>.
- Perez, F.F., Mourino, C., Fraga, F., Rios, A.F., 1993. Displacement of water masses and remineralization rates off the Iberian Peninsula by nutrient anomalies. J. Mar. Res. 51, 869–892. <https://doi.org/10.1357/0022240933223891>.
- Pingree, R.D., 2002. Ocean structure and climate (Eastern North Atlantic): in situ measurement and remote sensing (altimeter). J. Mar. Biol. Assoc. U. K. 82, 681–707. <https://doi.org/10.1017/S0025315402006082>.
- Pingree, R.D., 1993. Flow of surface waters to the west of the British isles and in the Bay of Biscay. Deep Sea Res. Part II Top. Stud. Oceanogr. 40, 369–388. [https://doi.org/10.1016/0967-0645\(93\)90022-F](https://doi.org/10.1016/0967-0645(93)90022-F).
- Pingree, R.D., Le Cann, B., 1989. Celtic and Armorican slope and shelf residual currents. Prog. Oceanogr. 23, 303–338. [https://doi.org/10.1016/0079-6611\(89\)90003-7](https://doi.org/10.1016/0079-6611(89)90003-7).
- Pingree, R.D., Sinha, B., Griffiths, C.R., 1999. Seasonality of the European slope current (Goban Spur) and ocean margin exchange. Continent. Shelf Res. 19, 929–975. [https://doi.org/10.1016/S0278-4343\(98\)00116-2](https://doi.org/10.1016/S0278-4343(98)00116-2).
- Pollard, R.T., Griffiths, M., Cunningham, S.A., Read, J., Pérez, F.F., Ríos, A.F., 1996. Vivaldi 1991-A study of the formation, circulation and ventilation of Eastern North Atlantic central water. Prog. Oceanogr. 37, 167–192. [https://doi.org/10.1016/S0079-6611\(96\)00008-0](https://doi.org/10.1016/S0079-6611(96)00008-0).
- Reid, J.L., 1979. On the contribution of the mediterranean Sea outflow to the Norwegian-Greenland sea. Deep sea research Part A. Oceanographic Research Papers 26, 1199–1223. [https://doi.org/10.1016/0198-0149\(79\)90064-5](https://doi.org/10.1016/0198-0149(79)90064-5).
- Rhein, M., Steinfeldt, R., Kieke, D., Stendardo, I., Yashayaev, I., 2017. Ventilation variability of Labrador Sea Water and its impact on oxygen and anthropogenic carbon: a review. Phil. Trans. Math. Phys. Eng. Sci. 375, 20160321 <https://doi.org/10.1098/rsta.2016.0321>.
- Schmitz Jr., W.J., McCartney, M.S., 1993. On the north Atlantic circulation. Rev. Geophys. 31, 29–49.
- Sherwin, T.J., Griffiths, C.R., Inall, M.E., Turrell, W.R., 2008. Quantifying the overflow across the Wyville Thomson Ridge into the Rockall Trough. Deep Sea Res. Oceanogr. Res. Pap. 55, 396–404. <https://doi.org/10.1016/j.dsr.2007.12.006>.
- Sherwin, T.J., Read, J.F., Holliday, N.P., Johnson, C., 2012. The impact of changes in North Atlantic Gyre distribution on water mass characteristics in the Rockall Trough. ICES (Int. Coun. Explor. Sea) J. Mar. Sci. 69, 751–757. <https://doi.org/10.1093/icesjms/fsr185>.
- Smilenova, A., Gula, J., Corre, M.L., Houpert, L., Reecht, Y., 2020. A persistent deep anticyclonic vortex in the Rockall Trough sustained by anticyclonic vortices shed from the slope current and wintertime convection. J. Geophys. Res.: Oceans 125, e2019JC015905. <https://doi.org/10.1029/2019JC015905>.
- Souza, A.J., Simpson, J.H., Harikrishnan, M., Malarkey, J., 2001. Flow structure and seasonality in the Hebridean slope current. Oceanol. Acta 24, 63–76. [https://doi.org/10.1016/S0399-1784\(00\)01103-8](https://doi.org/10.1016/S0399-1784(00)01103-8).
- Stendardo, I., Rhein, M., Steinfeldt, R., 2020. The North Atlantic current and its volume and freshwater transports in the subpolar North Atlantic, time period 1993–2016. J. Geophys. Res.: Oceans 125, e2020JC016065. <https://doi.org/10.1029/2020JC016065>.
- Talley, L.D., McCartney, M.S., 1982. Distribution and circulation of Labrador Sea Water. J. Phys. Oceanogr. 12, 1189–1205. [https://doi.org/10.1175/1520-0485\(1982\)012<1189:DACOLS>2.0.CO;2](https://doi.org/10.1175/1520-0485(1982)012<1189:DACOLS>2.0.CO;2).
- Thorpe, S.A., 1987. Current and temperature variability on the continental slope. Phil. Trans. Roy. Soc. Lond. Math. Phys. Sci. 323, 471–517.
- Ullgren, J.E., White, M., 2010. Water mass interaction at intermediate depths in the southern Rockall Trough, northeastern North Atlantic. Deep Sea Res. Oceanogr. Res. Pap. 57, 248–257. <https://doi.org/10.1016/j.dsr.2009.11.005>.
- van Aken, H.M., 2000. The hydrography of the mid-latitude northeast Atlantic Ocean: I: the deep water masses. Deep Sea Res. Oceanogr. Res. Pap. 47, 757–788. [https://doi.org/10.1016/S0967-0637\(99\)00092-8](https://doi.org/10.1016/S0967-0637(99)00092-8).
- Wade, I.P., Ellett, D.J., Heywood, K.J., 1997. The influence of intermediate waters on the stability of the eastern North Atlantic. Deep Sea Res. Oceanogr. Res. Pap. 44, 1405–1426. [https://doi.org/10.1016/S0967-0637\(97\)00023-X](https://doi.org/10.1016/S0967-0637(97)00023-X).
- White, M., Bowyer, P., 1997. The shelf-edge current north-west of Ireland. Presented at the Annales Geophysicae. Springer, pp. 1076–1083.
- Xu, W., Miller, P.L., Quartly, G.D., Pingree, R.D., 2015. Seasonality and interannual variability of the European Slope Current from 20 years of altimeter data compared with in situ measurements. Remote Sens. Environ. 162, 196–207. <https://doi.org/10.1016/j.rse.2015.02.008>.
- Yashayaev, I., Holliday, N.P., Bersch, M., van Aken, H.M., 2008. The history of the Labrador Sea Water: production, spreading, transformation and loss. In: Arctic-Subarctic Ocean Fluxes. Springer, pp. 569–612.
- Yashayaev, I., Loder, J.W., 2017. Further intensification of deep convection in the Labrador Sea in 2016. Geophys. Res. Lett. 44, 1429–1438. <https://doi.org/10.1002/2016GL071668>.
- Yashayaev, I., van Aken, H.M., Holliday, N.P., Bersch, M., 2007. Transformation of the Labrador Sea Water in the subpolar North Atlantic. Geophys. Res. Lett. 34 <https://doi.org/10.1029/2007GL031812>.